

Effects of Heat Treatments and Addition of Minor Elements of Boron and Nitrogen on Mechanical Properties and Microstructures of Reduced-Activation Ferritic/Martensitic Steel

Eiichi WAKAI, Masami ANDO, Nariaki OKUBO

Fusion R&D Directorate, Japan Atomic Energy Agency, Tokai-mura, Ibaraki, Japan

(Received: 30 September 2014 / Accepted: 19 January 2015)

Effects of heat treatments on the microstructures and mechanical properties of RAFM steels, including irradiation damage, were examined using the F82H steel and the F82H steel doped with boron and nitrogen. From a time of flight secondary ion mass spectroscopy (TOP-SIMS) analysis, it was found that a reheat treatment of the 2nd normalizing and tempering reduced the inhomogeneity of the material, and decreased the DBTT. Irradiation hardening and embrittlement of the F82H steel were changed by the initial tempering conditions before irradiation. It was also found that the DBTT shift can be reduced by the initial heat treatment and that the additions of minor elements of 60 wtppm ¹¹B and 200 wtppm nitrogen result in an effective reduction of irradiation embrittlement. The cause of reduction of irradiation embrittlement may be due to the formation of small BN clusters.

Keywords: F82H, RAFM, Heat treatment, Irradiation hardening, Irradiation embrittlement, DBTT, Tempering, Boron.

1. Introduction

The materials development of reduced-activation ferritic/martensitic (RAFM) steels for the fusion DEMO reactor was started around 1980s. Some important studies and evaluations for fusion reactor materials developments were performed [1-4], and the properties of Eurofer97 and IEA F82H are well known in general. RAFM steels are the first candidate materials for the first wall and blanket structure of fusion DEMO reactors, and the target back-plate and the target assembly of Irradiation Fusion Materials Irradiation facility (IFMIF). Recently, a new 5 tons F82H was produced in 2007 and 20 tons F82H was produced in 2011 under BA program [3-4]. In this study, several basic studies of radiation effects such as He and H on properties of materials are mainly evaluated, and the required materials properties for DEMO and IFMIF are also briefly introduced. In this study, there are two subjects as follows.

(1) Effect of initial heat treatment on the microstructures and mechanical properties of RAFM steels, including irradiation damage.

(2) Effects of additional minor elements of boron and nitrogen on the microstructures and mechanical properties of RAFM steels, including irradiation damage.

2. Effect of heat treatment on the microstructures and mechanical properties on RAFM steels

The irradiation hardening of RAFM steel changes depending on the irradiation temperature. The degradation of mechanical properties of RAFM steels induced by irradiation at around 300°C is thought to be mainly induced by the irradiation-hardening and -embrittlement. It is known that the irradiation hardening increases with irradiation dose, gradually saturating at about 50 dpa [5]. The increment of yield strength in Eurofer97 and F82H steels irradiated at 330°C reaches about 400 – 500 MPa, and the DBTT shift increases to 200 – 250°C by the neutron irradiation due to displacement damages [5]. In the temperature region above 400°C, the irradiation swelling of RAFM steels is induced [6-10].

Here, the factors of the irradiation hardening and the embrittlement are given as below.

(a) Factors of irradiation hardening

Formation of dislocation loops, cavities, black dot clusters and precipitates (M_6C , α' -precipitate, MX, etc.), the increment of dislocation density.

author's e-mail: wakai.eiichi@jaea.go.jp

Table 1 The chemical composition of the IEA heat F82H steel used in this study (wt%).

Alloy	B	N	Cr	W	C	O	Sol. Al	Si	P	S	Ti	V	Ni	Cu	Mn	Nb	Ta
F82H	0.0002	0.007	7.82	1.98	0.09	-	0.001	0.07	0.003	0.001	0.004	0.19	0.02	0.01	0.1	0.0002	0.04

Table 2 The chemical compositions of the other heat F82H steel and F82H+B and F82H+B+N steels used in this study (wt%).

	B	N	Cr	W	C	O	Al	Si	P	S	Ti	V	Mn	Ta
F82H	0.0002	0.0023	7.92	1.97	0.099	0.004	0.004	0.11	0.007	0.001	0.006	0.18	0.12	0.05
F82H+B	0.0059	0.0021	7.9	2.1	0.10	0.007	0.001	0.10	0.006	0.001	0.002	0.30	0.10	0.04
F82H+ ¹¹ B+N	0.0057	0.0200	7.83	2.09	0.099	<0.01	<0.001	0.10	0.006	0.001	0.002	0.30	0.10	0.042

(b) Factors of irradiation embrittlement

Irradiation hardening, the formation and growth of precipitates, and the degradation of the binding of boundaries due to irradiation-induced segregation of solute atoms and/or trapping of helium and hydrogen atoms on the boundaries, etc.

It was reported that the irradiation hardening and embrittlement of RAFM steels were less than those of the HT9 steel which was developed as a structural material for fast reactors [11]. Several types of RAFM steels were developed by several institutes, and the chemical elements are almost identical but the concentrations of the minor elements are also different. The heat treatments of RAFM steels for the tempering and normalizing are slightly different in each of RAFM steel. The difference in the response of mechanical properties such as embrittlement behaviors to neutron irradiation were estimated to be caused by the combined effects due to these differences [12]. The effects of tempering time and temperature on microstructures and mechanical properties in F82H steel were previously reported [13-19], and the method is very useful to control the materials properties and radiation resistance.

3. Experimental procedures

F82H steel used in this study is IEA heat and the other heat F82H, F82H+B, F82H+B+N steels, and the chemical compositions are given in Tables 1 and 2. In the IEA heat F82H, the heat treatments were normalized at 1040°C for 0.5 h and tempered at 750°C for 1 h, and the details were described in a reference [20]. In this study, additional heat treatments of re-normalizing and tempering were performed on the F82H steel. It was firstly re-normalized at 1040°C for 0.5 h in a vacuum, and it was cooled to room temperature. Then it was tempered at temperatures of 750, 780 and 800°C for 0.5 h in a vacuum. The tempering time at 750°C was varied between 0.5 and 10 h. The tensile test specimens of SS-3 type (gage size: 7.62 mm in length, 1.52 mm in width, 0.76 mm in thickness) were fabricated. Miniaturized

Charpy V-notched (CVN) impact (3.3 mm in width, 3.3 mm in height, 20 mm in length) specimens and 3mm-disk specimens for a TEM (a transmission electron microscope) observation were also fabricated. The Vickers hardness was measured at 10 kg by using a test machine of SHIMADZU co. Ltd., and Charpy impact tests were carried out using a test machine of JTT CIEM30D-01. Elemental distributions of Fe, B, C, N, Al, and P in the IEA F82H and the reheated F82H steel were measured by a time of flight-secondary ion mass spectroscope (TOF-SIMS) with 15 keV Ga⁺ ions over the scanned area of 100 × 100 μm after the pre-sputtering. The pre-sputtering was performed by 13 keV O⁺ ions and 25 keV Ga⁺ ions, for imaging the surface morphology and removing surface contamination, respectively. The microstructures were observed by a Hitachi HF-2000 of TEM operated at 200 kV.

The neutron irradiation was performed in the Japan Materials Test Reactor (JMTR) at 250°C to about 2 dpa.

4. Results of mechanical properties and microstructures in the reheated F82H

Fig. 1 shows Charpy impact energies as a function of test temperature in the IEA heat F82H steel before and after the reheat treatment (the second normalization: 1040°C for 0.5 h, the second tempering: 750°C for 1 h). The DBTT after the reheat treatment was decreased from

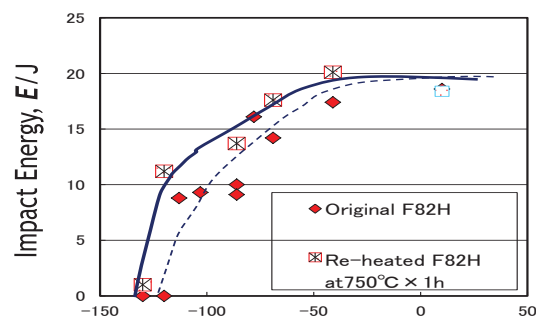


Fig. 1. Charpy impact energies of F82H steel before and after the reheat treatment (second normalization: 1040°C for 0.5 h, second tempering: 750°C for 1 h).

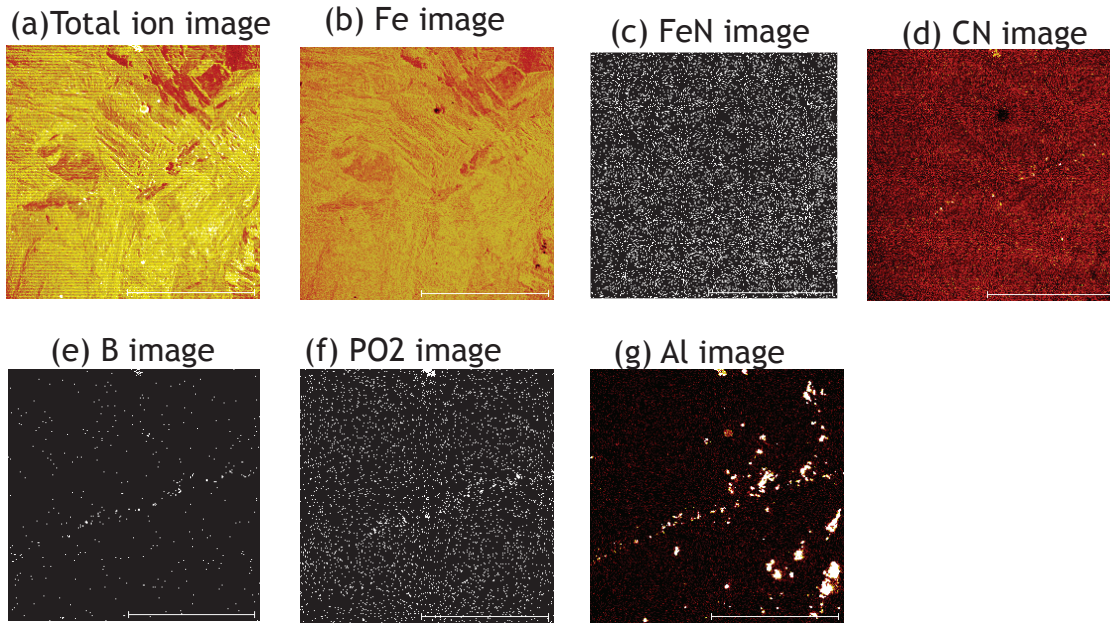


Fig. 2 SIMS images of the IEA heat F82H steel before the re-heat treatment.

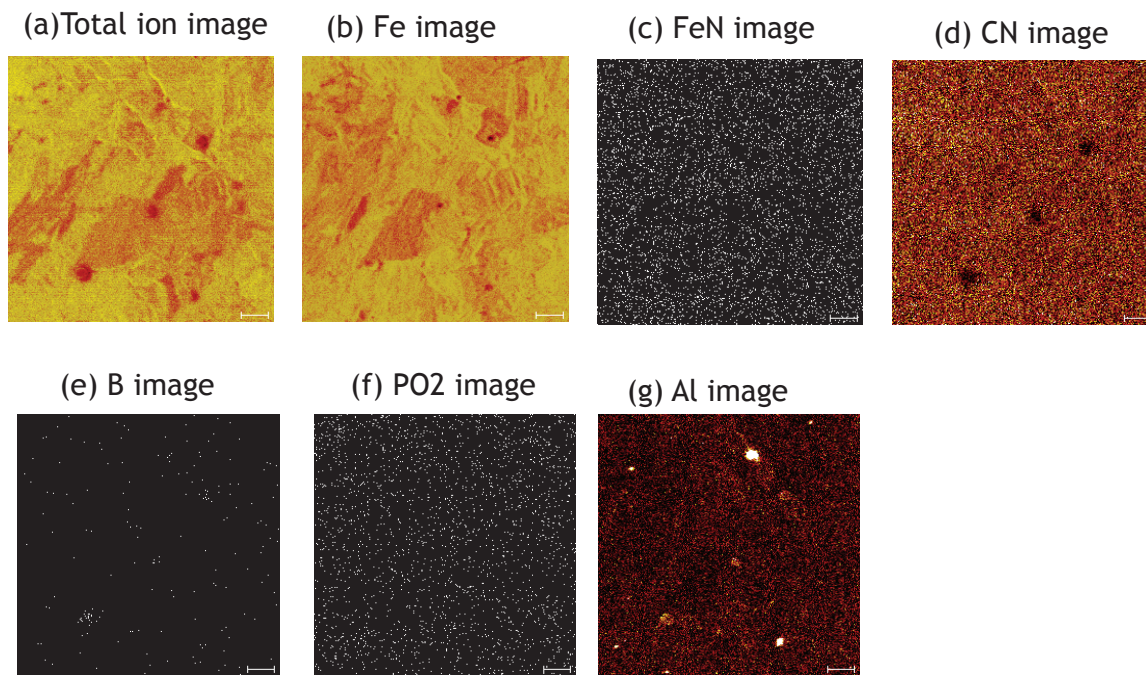


Fig. 3 SIMS images of the IEA heat F82H steel after the re-heat treatment.

about -100°C to about -120°C , and the DBTT of the IEA heat F82H steel was improved by the reheat treatment. To examine the cause of the improvement of DBTT, the distributions of some elements were measured by the TOP-SIMS. The SIMS images of the F82H steel before and after the re-heat treatment are shown in Figs. 2 and 3, respectively. The elements of B and P were segregated at the boundaries as seen in Fig. 2, and the precipitates of Al were observed in Fig. 2(g), which was in the localized

region of aluminum. The precipitates including aluminum element might be formed by the processing in the removal of oxygen using Al during the melting, and they are thought to be remained as aluminum oxide during the elimination process of oxides in the melting. By the reheat treatment, the isolated B distribution was reduced and the segregation of P disappeared, and the precipitates including Al were decreased.

The impact energies of 1/3 CVN specimens of F82H

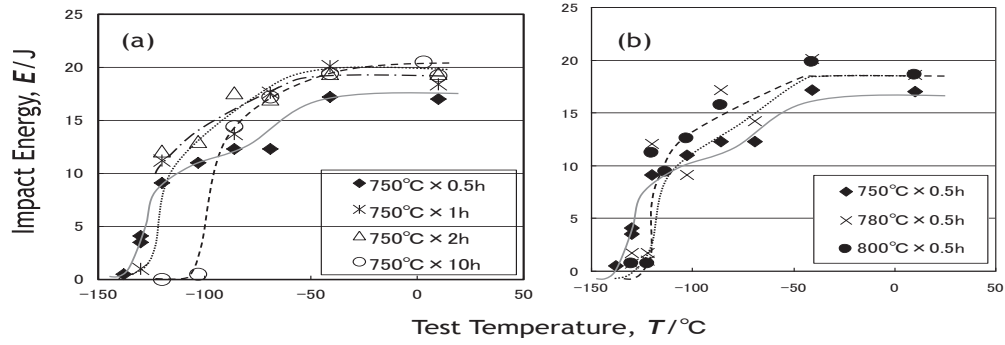


Fig. 4 Charpy impact energies of the F82H tempered at different conditions.

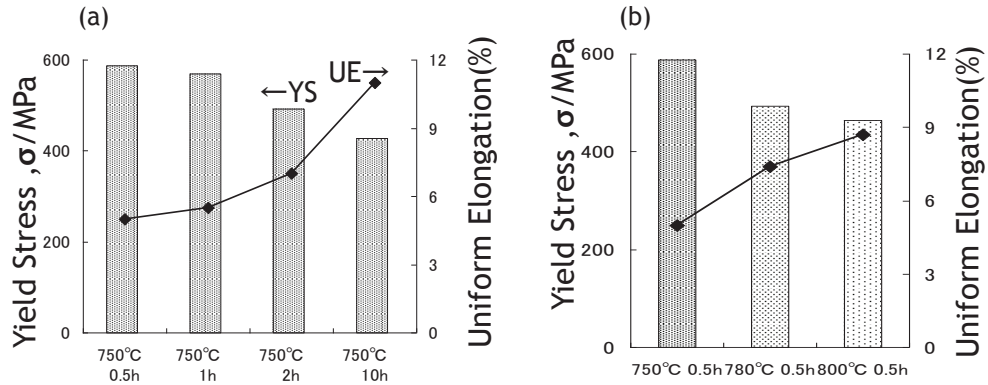


Fig. 5. Tensile properties of the re-heated F82H steel tempered at different times and temperatures.

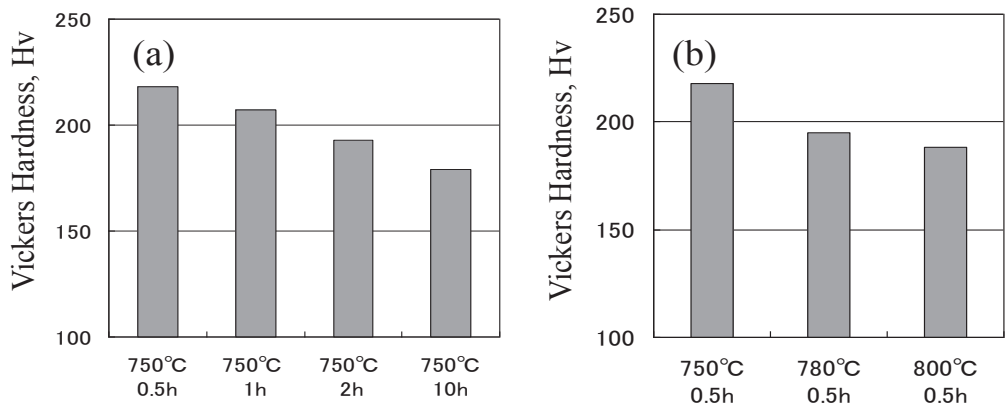


Fig. 6. Vickers hardness of the re-heated F82H steel tempered at different times and temperatures.

steel as a function of temperature are shown in Figs. 4(a) and (b). The highest DBTT was -94°C in the F82H steel tempered at 750°C for 10 h. DBTT of the specimens tempered at 750°C for 0.5 h, 1 h and 2 h was about -120°C as seen Fig. 4(a). DBTT of the specimens tempered at 780 and 800°C for 0.5 h was -104°C and -113°C , respectively, as given in Fig. 4(b).

Fig. 5 shows yield strengths and uniform elongations of F82H steels tempered at different conditions. The yield strength of the specimens decreased with increasing tempering temperature and time [9]. The Vickers hardness of the specimens was also given in Fig. 6. The Vickers hardness also decreased with increasing tempering temperature and time.

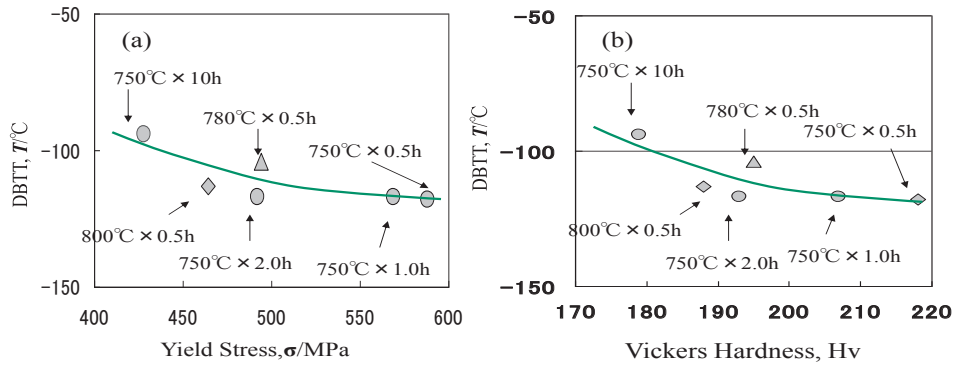


Fig. 7. The relations between DBTT [21] and yield stress or Vickers hardness in the reheated F82H steel tempered at different times and temperatures.

Fig. 7 shows the relations between DBTT and yield stress [21] and, DBTT and Vickers hardness in the reheated F82H steel tempered at different times and temperatures. In this heat treatment, the DBTT was not increased with the increment of the yield strength and Vickers hardness, but was roughly constant except for the lower region of the yield strength and Vickers hardness. The specimens with higher DBTT had relatively larger size carbides as shown in Figs. 9 and 10. Fig. 8 shows the relations between DBTT and yield stress in the other ferritic/martensitic steels, and the other ferritic/martensitic steels as shown in Fig. 8 had different concentrations in some elements and were tempered at different temperatures [22-29]. There was no correlation between the DBTT and the yield strength. The DBTT of the reheated F82H steel was lower than those of the other steels.

Figs. 9 and 10 show the microstructures of the reheated F82H steels. Lath martensitic structures with dislocations and carbides were observed in all specimens. Larger size carbides were observed in the specimen tempered at 750°C for 10 h as shown in Fig. 10(d). The slight growth of carbides of the F82H steel tempered at 780 and 800°C for 0.5 h were seen in Fig. 9.

It was reported that the IEA heat F82H was evaluated to include inhomogeneity, which was analyzed from the fracture behavior in the brittle-ductile transition temperature using the master curve analysis by M. Sokolov [29], and the large scattering of fracture toughness data in the brittle-ductile transition temperature region was shown in the study. The large scattering is thought to be induced by the inhomogeneity of the IEA heat F82H, and the inhomogeneity can be expected to be reduced effectively by the re-heat treatment shown in this study.

Irradiation experiments in the JMTR reactor at about 250°C to about 2 dpa was conducted for the reheated F82H steels as functions of tempering

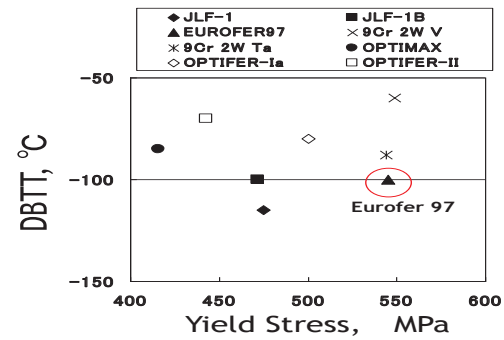


Fig. 8. The relations between DBTT and yield stress in the other ferritic/martensitic steels.

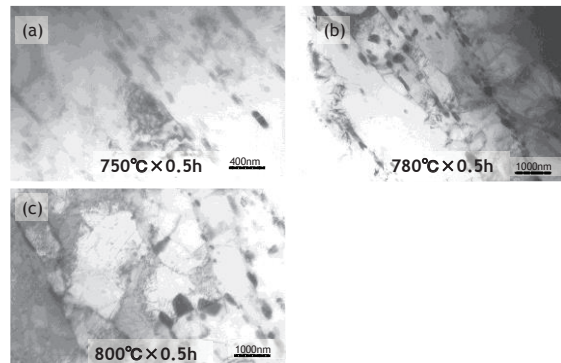


Fig. 9. Microstructures of F82H steel depending on the tempering temperatures.

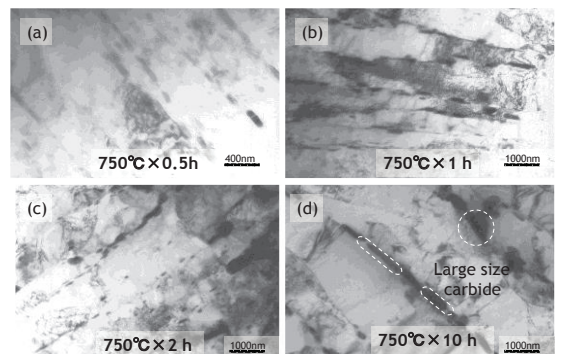


Fig. 10. Microstructures of F82H steel depending on the tempering time.

temperatures and times using the F82H steel of tensile specimens and Charpy impact specimens [13-17]. The DBTT shift due to the irradiation depended on the tempering conditions of time and temperature [15] as shown in Fig. 11. Thus, it was revealed that the irradiation hardening and embrittlement of RAF/M steel was strongly dependent on the heat treatment conditions before the irradiation. These results indicate that the change of carbon contents in the matrix and dislocation densities influenced by the heat treatments before the irradiation would affect the mobility of the point defects and the growth of defect clusters.

In order to reduce the DBTT shift by the neutron irradiation, further examination was conducted in a different approach using F82H steel doped with minor elements of boron (^{11}B) and nitrogen atoms. ^{11}B element has no nuclear reaction with thermal neutrons. The chemical compositions used in this experiment are given in Table 2. Figs. 12 (a) and (b) are phase diagrams of boron and nitrogen atoms in F82H steel calculated by the Thermo-Calc software. The phases in the boron and nitrogen elements as a function of temperature are shown in the figure. The heat treatments were conducted in two steps, and the first step normalizing was performed to prevent the formation of delta-ferrite and the following tempering was performed to suppress the formation of BN clusters in the specimen. The second normalizing was performed to adjust the grain size and also to form the BN clusters, and the second tempering was performed to form the carbides in the specimen. In the F82H+B+N steel, the procedures of the heat treatment are shown in Fig. 13. The previous research [30] showed that the boron examined by the SIMS using ^{42}BO ions was observed to be isolated in the F82H+60 wtpm-B steel under the same heat treatment with the IEA F82H steel as given in Fig. 14. The isolated size of boron was from a few μm to 20-30 μm .

In the present study, the distributions of boron, carbon, nitrogen and aluminum elements were measured by the TOP-SIMS. The TOP-SIMS images of the F82H steel, which was heat-treated with a condition of the minimum DBTT shift, and F82H+60 wtpm ^{11}B and F82H+60 wtpm ^{11}B + 200 wtpmN are given in Fig. 15. As shown in Fig. 15, slight isolations of boron were observed in the F82H steel, and the size was less than about 2 μm . The isolated position of boron corresponds to the position of aluminum. The position of aluminum is likely to correspond to oxides, not the carbides as seen in the ^{26}CN ion image. The behavior of the boron isolation was also observed in the F82H+60 wtpm-B and F82H+60 wtpm-B+200 wtpm-N. The intensity of the isolation boron increased in the F82H+60 wtpm-B, and

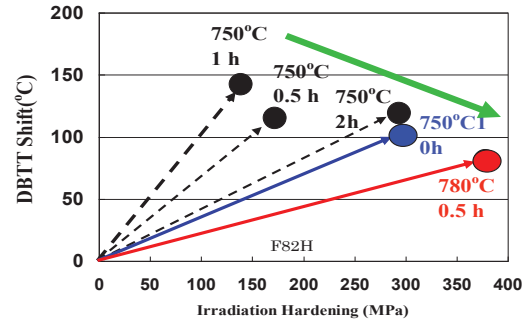


Fig. 11 Relation between the DBTT shift and irradiation hardening in the F82H depending on tempering conditions [15].

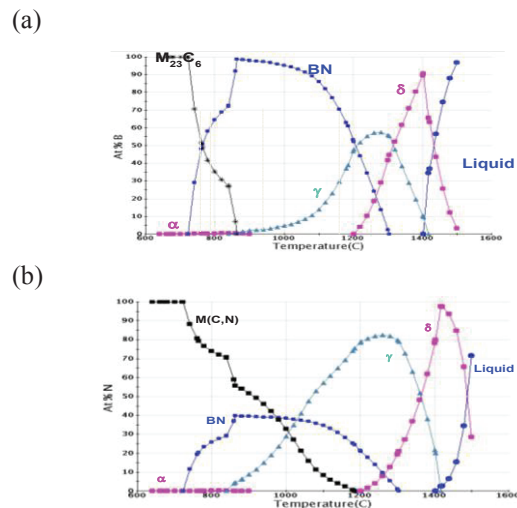


Fig. 12 The calculated positions for (a) boron and (b) nitrogen in F82H steel in the phase diagram.

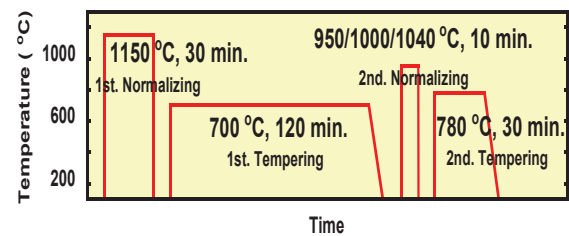


Fig. 13 Procedure of heat treatment of F82H+B, F82H+B+N and F82H .

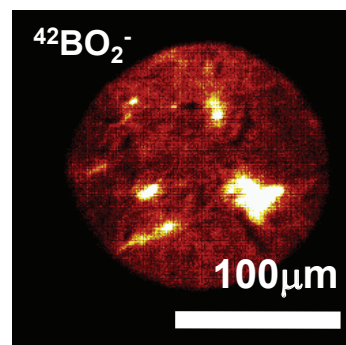


Fig. 14 SIMS image of F82H+60 wtpm B steel [21].

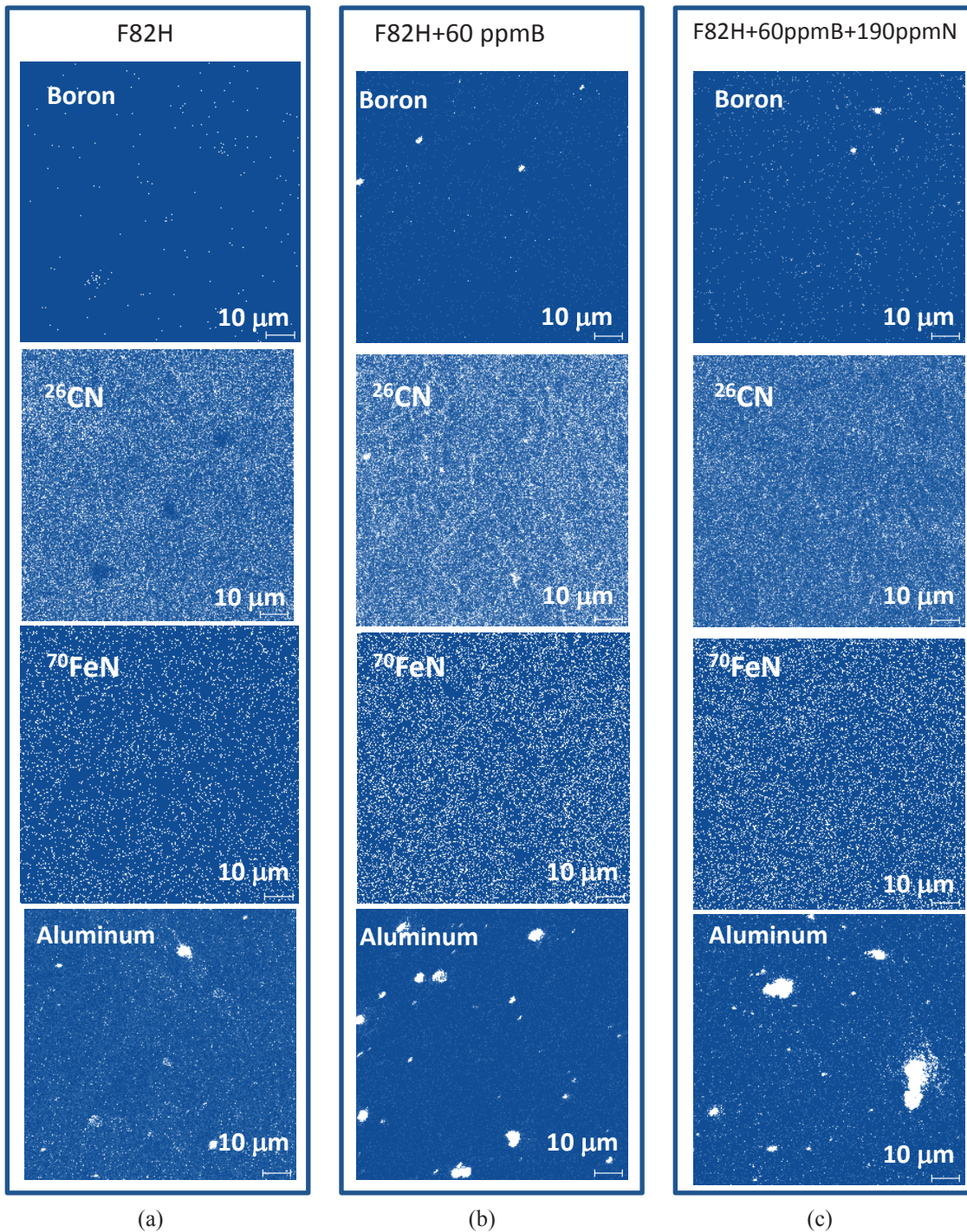


Fig. 15 TOP-SIMS images of boron and carbon elements (a) F82H, (b) F82H+60 ppmB, (c)F82H+60 ppmB+200 ppmN.

the numbers of the isolation boron was reduced in the F82H+60 wtppm-B+200 wtppm-N. The size of carbides in the F82H+60 wtppm-B increased. The larger size carbides may be induced by the absorption of boron element to $M_{23}C_6$ carbides due to the low content nitrogen in the F82H+60 wtppm-B steel as judged from Fig. 12(a).

However, in the improved heat treatment condition in this study, the isolated level in the F82H+60 wtppm ^{11}B was reduced as shown in Fig. 15(b), and the isolations of

the boron was very small in the F82H+60 wtppm ^{11}B +200 wtppmN as seen in Fig. 15(c). Microstructures of the F82H+60 wtppm ^{11}B +200 wtppmN steel and F82H steel tempered at 780°C for 0.5 h taken by a transmission electron microscope are shown in Fig. 16. The steel has a typical lath martensitic structure, and dislocations and carbides are seen. The size of carbides of the F82H steel were slightly larger than those of F82H+60 wtppm ^{11}B +200 wtppmN. Fig. 17 shows the reduction of DBTT shift in the F82H and F82H+60 wtppm ^{11}B +200 wtppmN steel tempered at 780°C for 0.5 h. The DBTT shift can be

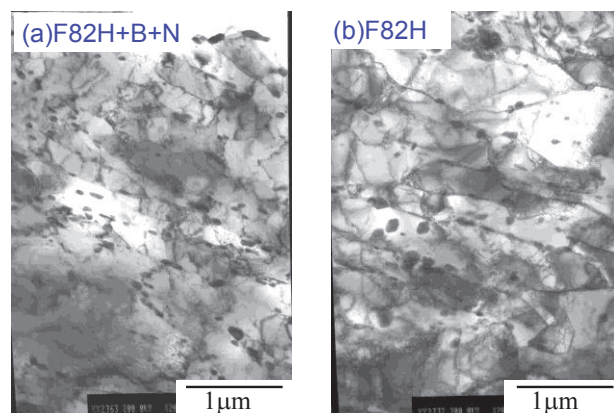


Fig. 16 Microstructures of (a) F82H+B+N and (b) F82H.

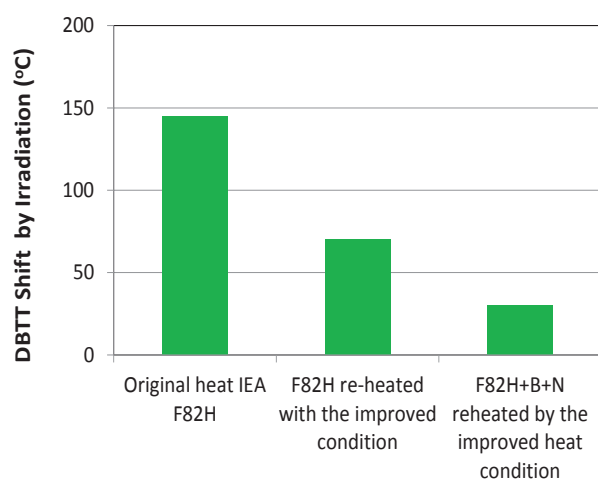


Fig. 17 DBTT shift due to irradiation in the IEA heat F82H, F82H with the reheated with the improved condition and F82H+B+N with the improved heat condition [15, 19].

reduced by the optimized heat conditions and the additions of minor elements of boron and nitrogen. The additional minor elements of ^{11}B and N to RAFM steels are very attractive for the radiation resistance. The BN clusters formed in the F82H steel can reduce the average of mobilities of point defects and may also act as sink sites for point defects. As the results, the irradiation hardening and embrittlement would be reduced.

The high dose irradiation experiment including the F82H+ ^{11}B +N steel is under conducting in the HFIR up to 80 dpa, and the results will be obtained within a few years later under a collaboration work of JAEA and DOE/ORNL.

5. Summary and Conclusion

In this study, the effects of initial heat treatments on the microstructures and mechanical properties of RAFM steels, including irradiation damage, were examined using the F82H steel and the F82H steel doped with 60 wtppm boron and 200 wtppm nitrogen.

From a time of flight secondary ion mass spectroscope (TOP-SIMS) analysis, the inhomogeneity of elements such as P, B, C, and N was measured, and the reheat treatment of the 2nd normalizing and tempering in the F82H steel reduced the inhomogeneity of material, and decreased the DBTT of the F82H. Irradiation hardening and embrittlement of the F82H steel changed by the initial tempering conditions before irradiation. It was found that the DBTT shift can be reduced by the initial heat treatment, and the additions of minor elements of 60 wtppm ^{11}B and 200 wtppm nitrogen resulted in an effective reduction of irradiation embrittlement. The BN clusters can reduce the average of mobilities of point defects and may also act as sink sites for point defects. As the results, the irradiation hardening and embrittlement would be reduced.

6. References

- [1] A.-A.F. Tavassoli *et al.*, *Fusion Eng. Des.* **61-62**, 617 (2002).
- [2] A.-A.F. Tavassoli *et al.*, *J. Nucl. Mater.* **329-333**, 257 (2004).
- [3] H. Tanigawa *et al.*, *Fusion Eng. and Des.* **86**, 2549 (2011).
- [4] H. Tanigawa *et al.*, *J. Nucl. Mater.*, **417**, 9 (2011).
- [5] E. Gaganidze *et al.*, *J. Nucl. Mater.*, **417**, 93 (2011).
- [6] T. Morimura *et al.*, *J. Nucl. Mater.*, **239**, 118 (1996).
- [7] E. Wakai *et al.*, *J. Nucl. Mater.*, **283-287**, 799 (2000).
- [8] E. Wakai *et al.*, *J. Nucl. Mater.*, **307-311**, 278 (2002).
- [9] E. Wakai *et al.*, *J. Nucl. Mater.*, **318**, 267 (2003).
- [10] E. Wakai *et al.*, *J. Nucl. Mater.*, **356**, 95 (2006).
- [11] A.F. Rowcliffe *et al.*, *J. Nucl. Mater.*, **258-263**, 1275 (1998).
- [12] M. Rieth *et al.*, *J. Nucl. Mater.*, **258-263**, 1147 (1998).
- [13] E. Wakai *et al.*, *J. Nucl. Mater.*, **329-333**, 1133 (2004).
- [14] E. Wakai *et al.*, *Mater. Trans.* **45**, 2638 (2004).
- [15] E. Wakai *et al.*, *Mater. Trans. JIM.* **46**, 481 (2005).
- [16] E. Wakai *et al.*, *Fusion Sci. Tech.*, **47**, 856 (2005).
- [17] N. Okubo *et al.*, *J. Nucl. Mater.*, **367-370**, 107 (2007).
- [18] E. Wakai *et al.*, *J. Nucl. Mater.*, **367-370**, 74 (2007).
- [19] E. Wakai *et al.*, *J. Nucl. Mater.*, **398**, 64 (2010).
- [20] K. Shiba *et al.*, *Properties of Low Activation Ferritic Steel F82H IEA Heat*, (JAERI-Tech 97-038, 1997, p. 117).
- [21] E. Wakai *et al.*, *Plasma and Fusion Research* **34**, 571, (2008).
- [22] E. van Osch *et al.*, *Effects of radiation on materials*, STP **1366**, 612 (2000).
- [23] R. L. Klueh and D. J. Alexander, *Effects of radiation on materials*, STP **1325**, 911, (1996).
- [24] A.F. Rowcliffe *et al.*, *J. Nucl. Mater.*, **258-263**, 1275,

- (1998).
- [25] A. Alamo, M. Horsten, X. Averty, E.I. Materna-Morris, M. Rieth and J.C. Brachet, *J. Nucl. Mater.*, **283-287**(2000)353.
 - [26] R.L. Klueh, M.A. Sokolov, K. Shiba, Y. Miwa and J.P. Robertson, *J. Nucl. Mater.*, **283-287**, 478, (2000).
 - [27] N. Blauc, RSchaublin, C. Bailat, F. Paschoud, M. Victoria, *J. Nucl. Mater.*,283-287, 731, (2000)..
 - [28] P. Saptig *et al.*, *J. Nucl. Mater.*, **367-370**, 527 (2007).
 - [29] M.A. Sokolov *et al.*, *J. Nucl. Mater.*, **367-370**, 587 (2007).
 - [30] E. Wakai *et al.*,*Mater. Trans. JIM.* **45**(8), 2642 (2004).